



## Hydrophobic ion pairing of a GLP-1 analogue for incorporating into lipid nanocarriers designed for oral delivery

Ruba Ismail<sup>a,b,1</sup>, Thi Nhu Quynh Phan<sup>c,d,1</sup>, Flavia Laffleur<sup>c</sup>, Ildikó Csóka<sup>a,b</sup>,  
Andreas Bernkop-Schnürch<sup>c,\*</sup>

<sup>a</sup> Institute of Pharmaceutical Technology and Regulatory Affairs, Institute of Pharmacy, University of Szeged, Eötvös u. 6, H-6720 Szeged, Hungary

<sup>b</sup> Institute of Pharmaceutical Technology and Regulatory Affairs, Interdisciplinary Centre of Excellence, University of Szeged, Eötvös u. 6, H-6720 Szeged, Hungary

<sup>c</sup> Department of Pharmaceutical Technology, Institute of Pharmacy, Leopold-Franzens-University Innsbruck, Innrain 80/82, 6020 Innsbruck, Austria

<sup>d</sup> Faculty of Pharmacy, University of Medicine and Pharmacy, Hue University, Thua Thien Hue, Viet Nam



### ARTICLE INFO

#### Keywords:

Hydrophobic ion pairing

HIP

Exenatide

GLP-1 analogue

Oral peptide drug delivery

Nanocarriers

Oral bioavailability

### ABSTRACT

The lipophilic character of peptides can be tremendously improved by hydrophobic ion pairing (HIP) with counterions to be efficiently incorporated into lipid-based nanocarriers (NCs). Herein, HIPs of exenatide with the cationic surfactant tetraheptylammonium bromide (THA) and the anionic surfactant sodium docusate (DOC) were formed to increase its lipophilicity. These HIPs were incorporated into lipid based NCs comprising 41% Capmul MCM, 15% Captex 355, 40% Cremophor RH and 4% propylene glycol. Exenatide-THA NCs showed a log  $D_{LPh/RM}$  lipophilic phase (LPh)/release medium (RM) of 2.29 and 1.92, whereas the log  $D_{LPh/RM}$  of exenatide-DOC was 1.2 and  $-0.9$  in simulated intestinal fluid and Hanks' balanced salts buffer (HBSS), respectively. No significant hemolytic activity was induced at a concentration of 0.25% (m/v) of both blank and loaded NCs. Exenatide-THA NCs and exenatide-DOC NCs showed a 10-fold and 3-fold enhancement in intestinal apparent membrane permeability compared to free exenatide, respectively. Furthermore, orally administered exenatide-THA and exenatide-DOC NCs in healthy rats resulted in a relative bioavailability of  $27.96 \pm 5.24\%$  and  $16.29 \pm 6.63\%$ , respectively, confirming the comparatively higher potential of the cationic surfactant over the anionic surfactant. Findings of this work highlight the potential of the type of counterion used for HIP as key to successful design of lipid-based NCs for oral exenatide delivery.

### 1. Introduction

Exenatide, a 39-amino-acid peptide (molecular mass: 4.186 kDa), shares a 50% sequence homology with the native GLP-1 with the substitution of amino acid Arg with Gly at the 2nd position providing resistance against DPP-4 and thus a longer half-life [1]. This GLP-1 analogue is marketed as Byetta® that is administered twice daily through subcutaneous (s.c.) injection, and as Bydureon® that is a sustained release product s.c. injected once-weekly [2]. Since frequent s.c. injection can adversely affect patients' adherence to the treatment, patient-friendly non-invasive delivery systems are highly on demand. The oral route is regarded as the most preferable choice due to high patient compliance in addition to mimicking the physiological GLP-1 secretion from the intestine to the systemic circulation [3–5]. Oral GLP-1 delivery, however, is limited by mainly two barriers: the harsh environment in the gastrointestinal tract (GIT) and the absorption membrane

barrier [6,7]. In September 2019 Novo Nordisk's semaglutide tablet (Rybelsus®) entered the global market as the first orally administered GLP-1 analogue formulation containing sodium N-(8-[2-hydroxybenzoyl] amino) caprylate as absorption enhancer. The absolute bioavailability of semaglutide, however, was estimated to be just 0.4%–1% after oral administration underlining the great dimension of these barriers [8].

Among the various technologies having been developed to overcome the obstacles limiting oral peptide delivery [9,10], the formation of hydrophobic ion pairs (HIPs) proved to be promising as this can increase the lipophilic character of hydrophilic peptide drugs and thus enhance their permeability of lipophilic membranes [11,12]. Because of a limited stability of HIPs in the GI tract, the incorporation of HIPs into lipophilic carrier systems is advantageous [13–15]. In addition to a protective effect towards presystemic metabolism [16–18], lipid-based nanocarrier systems in particular proved to be able to facilitate mucus

\* Corresponding author.

E-mail address: [andreas.bernkop@uibk.ac.at](mailto:andreas.bernkop@uibk.ac.at) (A. Bernkop-Schnürch).

<sup>1</sup> First authors.

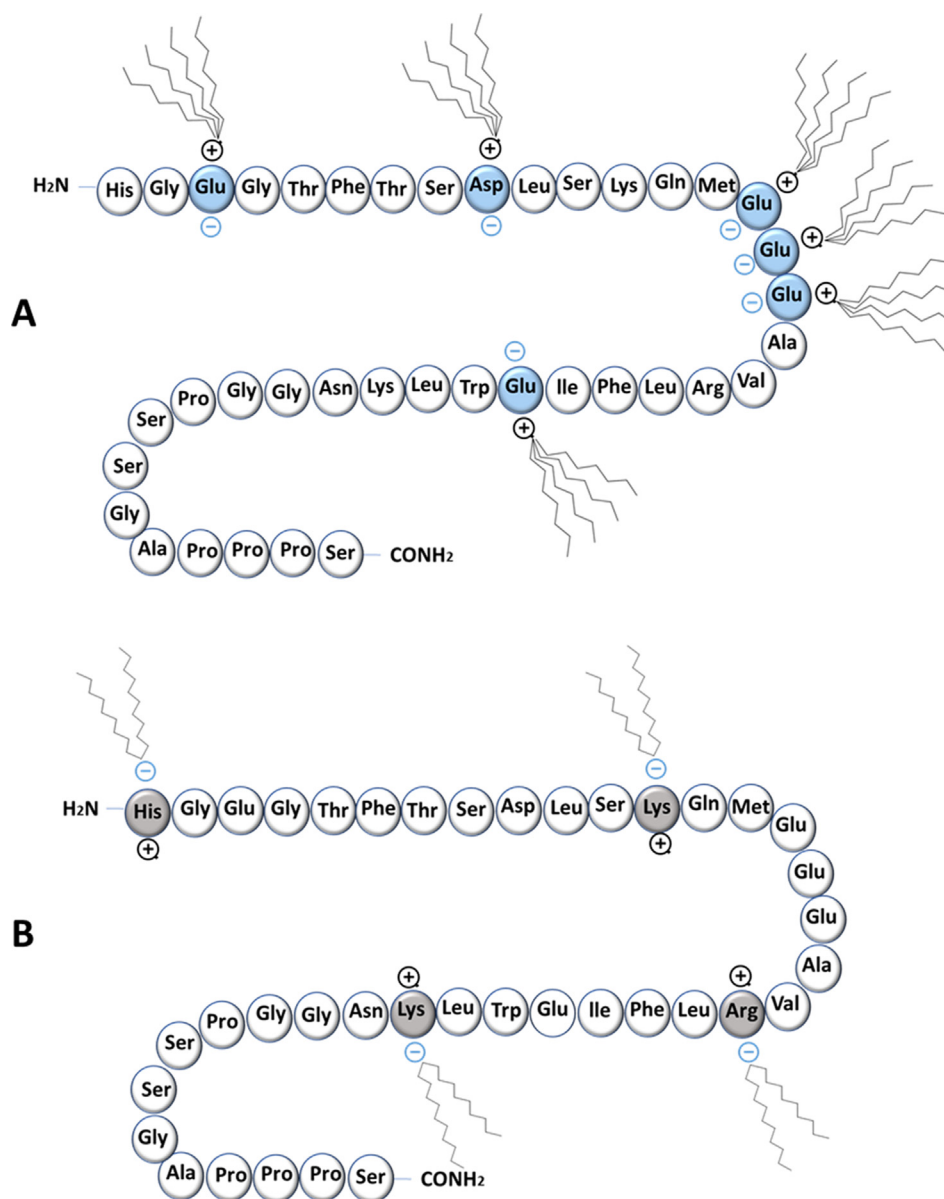


Fig. 1. The chemical structure of (A) exenatide-tetraheptylammonium bromide (THA) ion pairs, (B) exenatide-docusate (DOC) ion pairs.

permeation and to enhance the cellular uptake of peptides [19–22].

Various anionic surfactants were previously investigated by our research group regarding the formation of HIPs with exenatide, and exenatide-DOC ion pairs in a molar ratio of 1:4 were identified as most promising showing a relative oral bioavailability of 14% [23].

As exenatide bears not just cationic but also anionic substructures, it can likely form HIPs with cationic surfactants as well. Considering that there are four cationic amino acids but even six anionic amino acids on exenatide available for ion pairing as illustrated in Fig. 1, cationic surfactants might even show higher potential. Whether HIPs formed with cationic or anionic surfactant provide a higher bioavailability of exenatide, however, has not been investigated so far.

The aim of this research reported here was to investigate the potential of a cationic surfactant in forming HIPs with exenatide and to compare its efficacy with the most promising anionic surfactant docusate (DOC) [11,23]. Because of its permanent cationic charge and highly lipophilic character, tetraheptylammonium bromide (THA) having already shown potential for HIPs formation in a previous *in vivo* study was chosen [24]. Firstly, HIPs of exenatide-THA were optimized and the zeta potential change during HIPs formation was examined.

The most promising exenatide-THA and exenatide-DOC HIPs were incorporated in a lipid-based nanocarrier that was characterized regarding droplet size, polydispersity index (PDI) and zeta potential. Furthermore, safety and intestinal permeability of this delivery system was investigated, followed by pharmacokinetic studies in rats to evaluate their efficacy.

## 2. Materials and methods

### 2.1. Materials

Exenatide was purchased from Chemos GmbH (Germany). Capmul MCM EP (mono/diglycerides of caprylic acid, HLB 5–6) and Captex 355 (caprylic/capric triglycerides) were supplied by Abitec (USA). Cremophor RH (polyoxyl hydrogenated 40 castor oil, HLB 14–16), sodium docusate and tetraheptylammonium bromide were purchased from Sigma-Aldrich (Austria). Minimum Essential Medium Eagle (MEM) and Dulbecco's phosphate buffered saline (DPBS) were supplied from Biochrom GmbH, Berlin, Germany. Exendin-4 fluorescent ELISA kit was purchased from Phoenix Pharmaceuticals, Inc. (Burlingame,

CA). Hanks' Balanced Salts (HBSS), propylene glycol and all other reagents and solvents were purchased from Sigma -Aldrich (Austria).

## 2.2. Methods

### 2.2.1. Hplc

Reversed-phase HPLC (Hitachi Chromaster HPLC-system equipped with 5430 photodiode array UV detector, Tokyo, Japan) method was developed in our lab to quantify exenatide. A Nucleosil® C18 100–5 column (5 µm, 250\*4 mm, Phenomenex, USA) was used as stationary phase. The mobile phase consisted of 0.1% TFA in water (eluent A) and 80% acetonitrile with 0.1% TFA (eluent B), and was pumped in a linear-gradient mode from 58:42 (A:B, v/v) to 24:76 (A:B, v/v) at a flow rate of 0.75 ml/min over 22 min. The column temperature was set to 40 °C. Twenty microliters of sample volume was injected. The wavelength of UV detection was 278 nm. Retention time of exenatide was 16.5 min and the regression coefficient ( $R^2$ ) of calibration curve was 0.999 proving high linearity.

### 2.2.2. Hydrophobic ion-pairing of exenatide with THA and DOC

Exenatide acetate aqueous solution was prepared in a concentration of 2 mg/ml and pH was adjusted with 0.1 M NaOH to 8.0. Increasing amounts of THA were dissolved in 1 ml of demineralized water: methanol and added slowly and dropwise to 1 ml of the exenatide solution under light shaking. Exenatide to THA ratios of 1:1, 1:2, 1:4, 1:6, 1:8, 1:10 and 1:12 were tested. Exenatide-DOC ion pairs were prepared as previously described [23], where the pH of an exenatide solution of 2 mg/ml was adjusted to 3.0 with 2 M HCl followed by the addition of an equal volume of DOC aqueous solution slowly and dropwise to exenatide solution under light shaking. Exenatide to DOC molar ratios of 1:1, 1:2, 1:4 and 1:6 were tested.

HIPs were collected by centrifugation for 5 min at 13400 rpm (MiniSpin®, Eppendorf Austria GmbH) and washing 3 times with water. The supernatant that contained the remaining amount of dissolved exenatide was analyzed by HPLC as described above to calculate the precipitation efficiency using the following equation:

Precipitation efficiency(%)

$$= 100 - (\text{peptide concentration after HIP} / \text{peptide concentration before HIP} \times 100)$$

Zeta potential of HIPs with surfactant was determined with Zetasizer Nano ZSP (Malvern Instruments, Worcestershire, UK). Precipitated HIPs were frozen, freeze-dried at –30 °C and 3–5 mTorr (Christ Gamma 1–16 LSC Freeze dryer) and stored at –20 °C for further use.

### 2.3. Development and characterization of lipid-based nanocarriers

HIPs with THA were prepared in a molar ratio of 1:8 (exenatide:THA) at pH 8. HIPs with DOC were prepared in a molar ratio of 1:4 (exenatide:DOC) at pH 4 as previously described by our research group [23]. Lipid-based nanocarriers were formed by dissolving 2 mg of HIPs having been prepared as described above in 4 mg of propylene glycol (PG) by stirring for 2 min and homogenizing (1500 rpm) for 10 min at room temperature (Eppendorf ThermoMixer®, Hamburg, Germany). This was followed by addition of 41 mg of Capmul MCM (oil), 40 mg of Kolliphor RH (surfactant) and 15 mg of Captex 355 (oil) and homogenizing the mixture (1500 rpm) after the addition of each component (Eppendorf ThermoMixer®, Hamburg, Germany).

To determine the maximum payload of HIPs and exenatide in the formulation, the preconcentrate was analyzed by HPLC. Furthermore, size, polydispersity index and zeta potential of NCs having been dispersed in demineralized water (1:100) were measured via Zetasizer Nano ZSP (Malvern Instruments, Worcestershire, UK). Aiming to assess the stability of the NCs, droplet size, PDI and zeta potential were

measured after 4 h and one week.

### 2.4. Determination of $\log D_{\text{lipophilic phase (LPh)}/\text{release medium (RM)}}$ of exenatide-THA and exenatide-DOC

The release characteristics of exenatide-THA and exenatide-DOC from the nanocarriers were evaluated by determining the distribution of the ion pairs between the lipophilic phase of the NCs and the release medium ( $\log D_{\text{LPh/RM}}$ ) [25,26]. Lyophilized exenatide-THA (molar ratio 1:8) and exenatide-DOC (molar ratio 1:4) were dispersed in simulated intestinal fluid (50 mM phosphate buffer pH 6.8), HBSS and the lipophilic phase of the NC. After stirring for 3 h at 1000 rpm, each suspension was centrifuged for 5 min at 13,400 rpm. The solubility of HIPs in each release medium ( $C_{\text{RM}}$ ) and the lipophilic phase of the nanocarrier ( $C_{\text{LPh}}$ ) was calculated by analyzing the supernatant by HPLC.  $\log D_{\text{LPh/RM}}$  of HIPs was calculated according to the following equation:

$$\log D_{\text{LPh/RM}} = \log \frac{C_{\text{RM}}}{C_{\text{LPh}}}$$

### 2.5. In vitro hemolysis assay

In vitro hemolysis assay with exenatide-THA and exenatide-DOC as well as blank NCs was performed according to a previously reported protocol [27]. The dilution of 0.556 ml of human whole blood with 1.944 ml of sterile Dulbecco's PBS pH 7.4 was performed. Subsequently, 1 ml of this suspension was diluted with 49 ml of sterile Dulbecco's PBS pH 7.4.

First, 50 µl of NCs was added to 1 ml of diluted blood to the final concentration of 0.1%, 0.25% and 0.5% (m/v). This was followed by an immediate shaking of the mixtures on thermomixer for 2 h at 300 rpm and 37 °C and additionally homogenized by inversion during the incubation. Then, the mixtures were centrifuged at 503\*g for 5 min at 5 °C. Tecan infinite M200 plate reader was used to read the absorbance of the supernatants at a wavelength of 420 nm. Triton-X-100 1% (m/v) in MEM and sterile Dulbecco's PBS pH 7.4 served as positive and negative control, respectively.

The percentage of hemolysis (H %) was calculated as follows:

$$H(\%) = \frac{\text{Abs}(\text{test}) - \text{Abs}(\text{neg})}{\text{Abs}(\text{pos}) - \text{Abs}(\text{neg})}$$

where  $\text{Abs}_{\text{test}}$  is absorbance of the test sample,  $\text{Abs}_{\text{neg}}$  is absorbance of PBS (negative control) and  $\text{Abs}_{\text{pos}}$  is absorbance of Triton-X-100 (positive control).

### 2.6. Ex vivo permeability study

The ex-vivo permeability study was carried out on fasted rats with a body weight of 200–250 g. Rats were sacrificed and the freshly excised small intestine was preincubated in HBSS buffer for 30 min before being cut into strips of 2 cm mounted in Ussing-type chambers. The apical and basolateral sides were filled with 1 ml of HBSS pH 6.8 and incubated for 30 min in a water bath at 37 °C. Then, HBSS was replaced by fresh incubation medium at apical side and by the following test samples: (1) 0.25% of exenatide-THA-NCs, (2) 0.6% of exenatide-DOC NCs and (3) 8 µg /ml of exenatide solution in HBSS at the apical side.

Aliquots of 200 µl were withdrawn from the basolateral side at 1, 2, and 3 h and replaced with an equal volume of fresh HBSS preincubated at 37 °C. Exenatide concentration in the aliquots was quantified by fluorescent ELISA immunoassay (FEK-070-94; Phoenix Pharmaceuticals, Inc., USA) following the manufacturer's instructions. The absorbance was read at 450 nm using a microplate reader (Spark Multimode microplate reader, Tecan). Values are presented as means ± SD ( $n = 3$ ).

## 2.7. In vivo study

Male Sprague-Dawley rats with a body weight of 200–250 g were supplied by Janvier Labs (Saint Berthevin, France) and the *in vivo* study was approved by the Ethical Committee of Austria and performed according to the principles of Laboratory Animal Care.

Rats were fasted 2 h prior to drug administration and 6 h thereafter but had free access to water during the entire experiment. Rats were divided into four groups ( $n = 5$ ). A dose of 50  $\mu\text{g}/\text{kg}$  body of exenatide solution was administered to the first group via subcutaneous injection. The second group was the negative control group where exenatide solution was orally administered at a dose of 300  $\mu\text{g}/\text{kg}$  body. The third and fourth group received 300  $\mu\text{g}/\text{kg}$  body weight of exenatide-THA and exenatide-DOC NC formulation via oral gavage, respectively. The formulations were diluted with water (1:2) before administration.

Blood samples (100  $\mu\text{l}$ ) were collected from the tail vein before drug administration and at predetermined time points after dosing. Following the centrifugation of the blood samples for 5 min at 2000 $\times$ g and 4  $^{\circ}\text{C}$ , the serum was separated and stored at  $-80^{\circ}\text{C}$  for further analysis. Exenatide concentration was measured by fluorescent ELISA immunoassay (FEK-070-94; Phoenix Pharmaceuticals, INC., USA). The absorbance was read at 450 nm using a microplate reader (Spark Multimode microplate reader, Tecan).

The relative bioavailability ( $\text{BA}_R$ ) of exenatide after oral administration was calculated using the following equation:

$$\text{BA}_R(\%) = \frac{\text{AUC (oral)} \times \text{Dose (S.C.)}}{\text{AUC (S.C.)} \times \text{Dose (oral)}} \times 100$$

## 2.8. Statistical analysis

The GraphPad Prism software (version 5.0.1) was used to conduct the statistical data analysis, performing Analysis of Variance (ANOVA) followed by Bonferroni test with  $p < 0.05$  as the minimal level of significance. All values are shown as means  $\pm$  SD.

## 3. Results

### 3.1. Hydrophobic ion-pairing of exenatide with cationic/anionic surfactants

The cationic surfactant THA and the anionic surfactant DOC were capable of forming HIPs with the anionic and cationic amino acids of exenatide via non-covalent ionic interactions (Fig. 1). The addition of THA or DOC to the exenatide solution caused an immediate precipitation indicating the formation of HIPs. Different exenatide to surfactant ratios were evaluated as illustrated in Fig. 2. The more surfactant was added to exenatide, the more HIPs were formed until the maximum precipitation efficiency of  $95.3 \pm 4.02\%$  at molar ratio of 1:8 (exenatide: THA), whereas a maximum of 100% was reached in case of DOC at molar ratio of 1:4 (exenatide: DOC). Higher concentrations of surfactant led to a lower amount of formed ion pairs. This observation was previously also reported for other surfactants [11] and could be due to the formation of micelles that re-dissolve the ion pair complex [28].

### 3.2. Zeta potential of exenatide-surfactant HIPs

The zeta potential of HIPs having been formed at different molar ratios of exenatide to surfactant was tested in order to evaluate the surface charge of the complexes. Fig. 3A shows that the negative charge of exenatide at pH 8.0 decreased with the increase in THA having been bound to the peptide drug reaching the lowest negative zeta potential at a molar ratio of 1:10 (exenatide: THA). At a higher molar ratio, the THA level could exceed the critical micellar concentration (CMC) and the resulting formation of micelles can explain the increase in negative zeta potential due to the solubilizing effect of the excess of THA. The

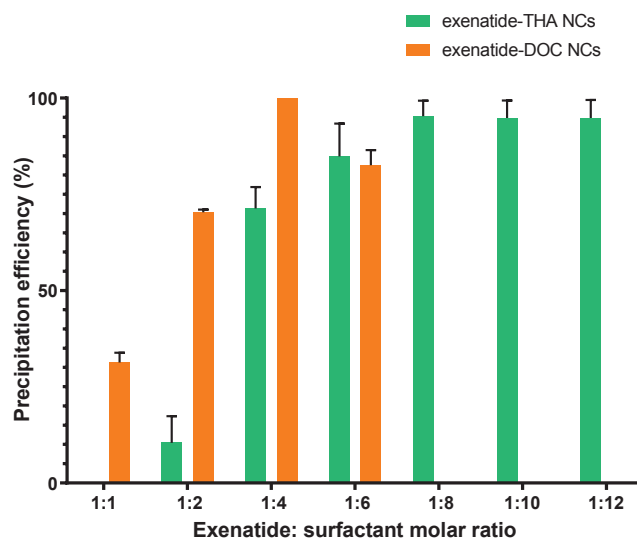


Fig. 2. Precipitation efficiency of exenatide (2 mg/mL) with THA and DOC at different molar ratios. The precipitated exenatide-surfactant ion pairs were centrifuged and the remaining amount of exenatide in supernatant was quantified by HPLC. Data are presented as mean  $\pm$  SD ( $n = 3$ ).

formation of these micelles could attribute to reduce the amount of THA being bound to the surface of exenatide causing a higher negative charge. In case of exenatide-DOC, a shift in zeta potential toward negative values was observed where the positive charge of exenatide at pH 3.0 decreased with higher molar ratio (exenatide:DOC) reaching almost 0 mV at a molar ratio of 1:4 (Fig. 3B).

## 4. Development and characterization of the nanocarrier system

The maximum payload of exenatide-THA and exenatide-DOC that could be dissolved in the lipophilic phase of the NCs was 0.54% and 0.17%, respectively. This payload was used to prepare NCs for further evaluation.

Small droplet size ( $< 30$  nm) with low PDI value was determined for blank and loaded NCs (Table 1). The surface charge of exenatide-THA loaded NCs was positive whereas negative values were measured in case of exenatide-DOC loaded NCs. This observation can be explained by the cationic character of THA and the anionic character of DOC. Both blank and loaded NCs showed sufficient stability for one week regarding the droplet size, PDI and zeta potential as shown in Table 1.

### 4.1. Determination of log D of exenatide-THA and exenatide-DOC

It was previously reported that the drug release from lipid-based NCs formulation depends on a simple diffusion process from a lipophilic liquid phase into an aqueous liquid phase that occurs within a few seconds [26]. As the released HIPs are absorbed from the membrane, more HIPs will diffuse out of the nanodroplets until equilibrium is reached again. Since drug release is controlled by the partition coefficient of HIPs between the lipophilic phase (LPh) and the release medium (RM) that should mimic gastrointestinal conditions,  $\log D_{LPh/RM}$  was determined in two different aqueous media [25,26].  $\log D_{LPh/RM}$  of exenatide-THA was 2.29 and 1.92, whereas the  $\log D_{LPh/RM}$  of exenatide-DOC was 1.2 and  $-0.9$  in simulated intestinal fluid and HBSS, respectively. These log D values proved that THA is capable of forming more pronounced hydrophobic complexes than DOC.

### 4.2. Cytocompatibility

The *in vitro* hemolysis assay on human erythrocytes can be used as a rapid and reliable method to evaluate the effect of drug delivery

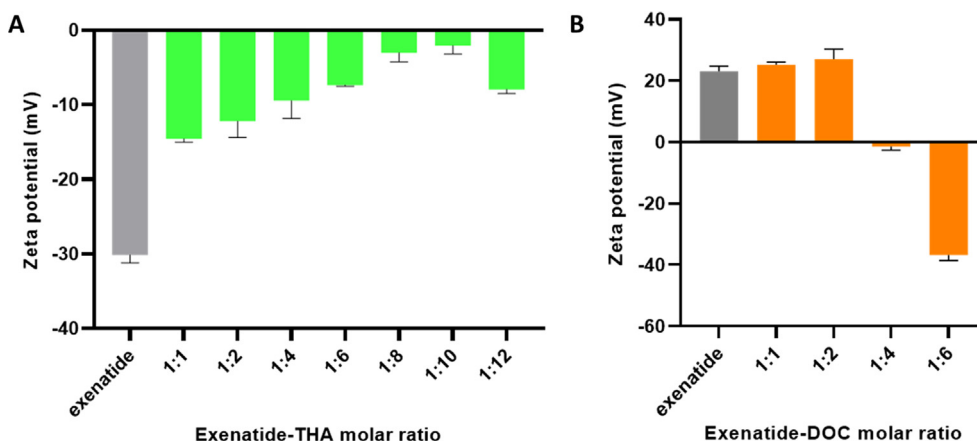


**Fig. 3.** The shift in zeta potential values of (A) exenatide-THA HIPs formed at pH 8.0 in different molar ratios, (B) exenatide-DOC HIPs formed at pH 3.0 in different molar ratios. Data are presented as mean  $\pm$  SD ( $n = 3$ ).

**Table 1**

Droplet Size, polydispersity index (PDI), zeta potential of blank NCs, exenatide-THA N.

	Droplet Size (nm)	PDI	Zeta potential (mV)
<b>0 h</b>			
Exenatide-THA NCs	25.71 $\pm$ 2.48	0.24 $\pm$ 0.48	10.11 $\pm$ 1.07
Exenatide-DOC NCs	24.55 $\pm$ 3.2	0.25 $\pm$ 0.046	20 $\pm$ 2.2-
Blank NCs	24.11 $\pm$ 2.26	0.13 $\pm$ 0.04	3.42 $\pm$ 0.47-
<b>4 h</b>			
Exenatide-THA NCs	23.64 $\pm$ 2.75	0.05 $\pm$ 0.03	5.5 $\pm$ 0.85
Exenatide-DOC NCs	25.17 $\pm$ 5.22	0.2 $\pm$ 0.07	12.67 $\pm$ 2.08-
Blank NCs	26.24 $\pm$ 1.61	0.04 $\pm$ 0.02	2.5 $\pm$ 1.07-
<b>1 week</b>			
Exenatide-THA NCs	22.49 $\pm$ 4.55	0.081 $\pm$ 0.11	9.24 $\pm$ 3.42
Exenatide-DOC NCs	20.2 $\pm$ 0.63	0.11 $\pm$ 0.05	9.37 $\pm$ 0.15-
Blank NCs	27.07 $\pm$ 1.76	0.13 $\pm$ 0.06	7.3 $\pm$ 0.38-

Gs and exenatide-DOC NCs in water over time. Data are presented as mean  $\pm$  SD ( $n = 3$ ).

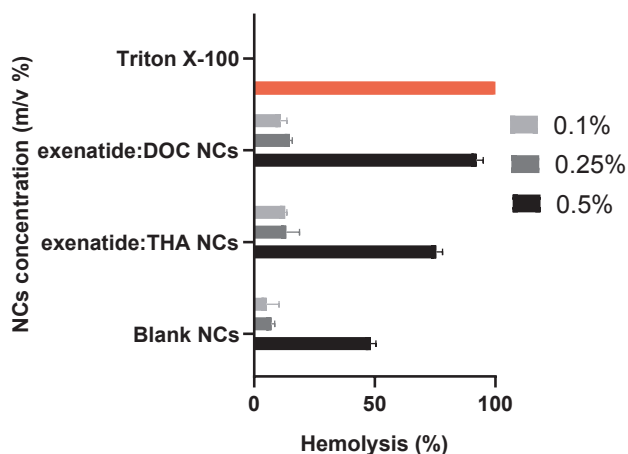


**Fig. 4.** Cytotoxicity of different concentrations of blank NCs, exenatide-THA NCs, exenatide-DOC NCs. Hemolysis assay was conducted with human red blood cells (RBC). Data are presented as mean  $\pm$  SD ( $n = 3$ ).

systems on cell membranes [27,29]. In comparison to other cell types, the cell membrane of erythrocytes is very fragile. NCs loaded with different concentrations of either exenatide-THA or exenatide-DOC were tested regarding their hemolytic activity and compared to blank NCs. Fig. 4 displays the hemolysis caused by increasing concentrations of blank and loaded NCs. Compared to NCs loaded with exenatide-THA,

NCs loaded with exenatide-DOC showed higher toxicity as concluded from the hemolytic activity reaching more than 90% at a concentration of 0.5% (m/v) of this formulation.

#### 4.3. Ex-vivo permeability study

Results presented in Fig. 5 clearly demonstrated that the intestinal permeation of exenatide incorporated in NCs was enhanced in comparison to the free peptide. Moreover, results proved the superiority of exenatide-THA NCs when compared to exenatide-DOC NCs. This outcome provides evidence for the crucial role of the type of HIPs incorporated in NCs in enhancing permeability across the intestinal mucus gel layer and epithelial barrier strongly limiting oral peptide uptake.

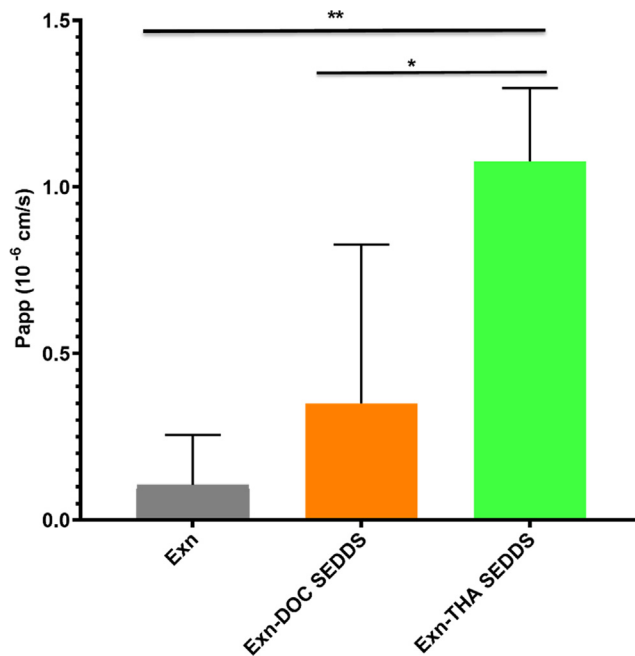


**Fig. 5.** Evaluation of ex vivo permeability of exenatide across rat intestinal mucosa following the treatment with free exenatide solution, exenatide-THA NCs or exenatide-DOC NCs. Values are presented as means  $\pm$  SD ( $n = 3$ ). Statistical analysis: Analysis of Variance (ANOVA) followed by Bonferroni test, \*  $p < 0.05$ , \*\*  $P < 0.01$ .

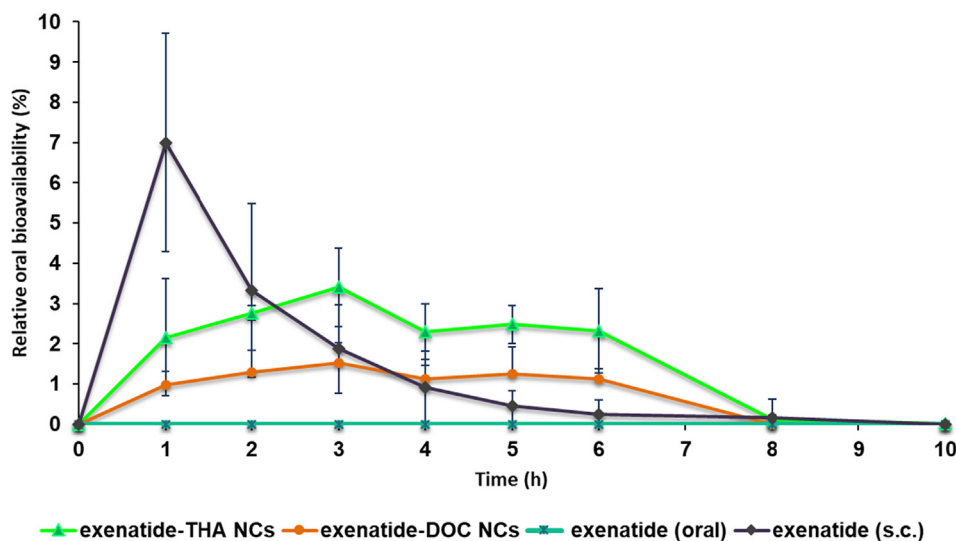


Fig. 6. Exenatide plasma concentration vs time profiles for s.c. free exenatide solution (50  $\mu\text{g}/\text{kg}$ ), oral exenatide solution (dose: 300  $\mu\text{g}/\text{ml}$ ), oral exenatide-THA NCs (dose: 300  $\mu\text{g}/\text{ml}$ ) and oral exenatide-DOC NCs (dose: 300  $\mu\text{g}/\text{ml}$ ). Values are presented as means  $\pm$  SD ( $n = 5$ ).

#### 4.4. In-vivo study

As illustrated in Fig. 6, s.c. injection of free exenatide solution elicited a maximum serum level at 1 h after administration being in good agreement with previous reported studies [30]. The orally administered free exenatide solution could not provide any systemic uptake of the drug. In contrast, high exenatide serum levels were observed after oral administration of exenatide-THA and exenatide-DOC NCs reaching maximum after 3 h. The relative oral bioavailability (versus s.c.) of exenatide-THA NCs (Table 2) was  $27.96 \pm 5.24\%$ . This is to our knowledge the highest so far achieved oral bioavailability of a GLP-1 analogue emphasizing the great potential of hydrophobic ion pairing for oral peptide delivery. The oral bioavailability of the exenatide-THA ion pair was almost 2-fold higher than that of the exenatide-DOC ion pair (Table 2). These results were in good accordance with the permeation behaviour of these HIPs on the intestinal mucosa as shown in Fig. 5 demonstrating a 3-fold higher  $P_{app}$  of the exenatide-THA ion pair.

## 5. Discussion

Despite the advances in peptide and protein delivery, the oral delivery of GLP-1 analogues like exenatide is still an elusive goal being limited by mainly the enzymatic barrier, mucus barrier and low membrane permeability. In this study, exenatide was incorporated in lipid-based NCs since it has been proven in many previous studies that lipid-based NCs can overcome the above mentioned hurdles for oral peptide delivery [7,16,22]. Hydrophobic ion pairing was applied before

Table 2

Pharmacokinetic parameters of exenatide in rats following s.c. injection of the free exenatide solution and oral administration of exenatide solution, exenatide-THA NCs and exenatide-DOC NCs.  $C_{max}$ : maximum serum concentration;  $T_{max}$ : time at which  $C_{max}$  is reached; AUC 0–10: area under the serum concentration-time curve over 10 h,  $BA_R$ : relative bioavailability ( $n = 5$ ).

Formulation	Free exenatide solution	Exenatide-THA NCs	Exenatide-DOC NCs
Route of administration	s.c.	oral	oral
Dose ( $\mu\text{g}/\text{Kg}$ )	50	300	300
$C_{max}$ (ng/ml)	$7.0 \pm 2.70$	$3.4 \pm 0.97$	$1.53 \pm 0.50$
$T_{max}$ (h)	1	3	3
AUC 0–10 (ng h/ml)	$10.56 \pm 3.92$	$17.33 \pm 3.48$	$10.28 \pm 4.7$
$BA_R$ (%)	100	$27.96 \pm 5.24$	$16.29 \pm 6.63$

incorporation in NCs to sufficiently reduce hydrophilicity of the peptide by masking its ionic substructures with bulky lipophilic counter-ions [17,21,31]. The isoelectric point (IP) of exenatide is 4.86 [32]. At a pH above this IP the drug bears six anionic substructures at position 3, 9, 15, 16, 17 and 24 in its amino acid sequence being available for ion pairing with the cationic surfactant THA. The highest ion-pairing efficiency was reached at a molar ratio of 1:8 (exenatide: THA) and pH adjusted to 8.0 (Fig. 2). In contrast, at pH below the IP of exenatide, the peptide bears 4 cationic substructures in its amino acid sequence at position 1, 12, 20 and 27 being capable of forming ion pairs with the anionic surfactant DOC. Exenatide-DOC ion pairs had the highest precipitation efficiency at a molar ratio of 1:4 (exenatide: DOC) and pH adjusted to 3.0.

The formation of HIPs with THA and DOC was further confirmed by a shift in zeta potential showing a clear trend to less negative values the more THA was bound to exenatide, whereas a clear trend to less positive values the more DOC was bound to the drug (Fig. 3).

For the development of NCs, an as low as feasible concentration of PG was used to dissolve HIPs in NCs, as this hydrophilic co-solvent is immediately released from the lipophilic phase in aqueous media promoting the release of HIPs out of the oily droplets [14]. Exenatide release from NCs was characterized based on the affinity of HIPs toward the oily phase of NCs and the release medium [25]. A log D of at least 2 has been demanded to keep  $\geq 50\%$  of HIPs in NCs [14]. Our results showed that exenatide-THA HIPs with a log D of 2.29 were superior to exenatide-DOC with a log D of 1.2 in SIF. Accordingly, the amount of exenatide immediately released from exenatide-DOC NCs is likely higher than that from exenatide-THA NCs.

In vitro toxicity studies with human red blood cells (RBC) revealed that both blank and loaded NCs displayed no significant hemolytic activity at concentrations of 0.1% (m/v) and 0.25% (m/v). However, the hemolytic activity was higher at 0.5% (m/v) of NCs confirming that this toxicity is concentration dependent, reaching more than 70% and 90% in exenatide-THA NCs and exenatide-DOC NCs, respectively (Fig. 4). The concentration of 0.25% (m/v) was selected for further investigations. Exenatide-DOC NCs and exenatide-THA NCs showed a 3-fold and 10-fold enhancement in intestinal membrane permeability compared to free exenatide (Fig. 5). The lipophilic nature of NCs and their slippery surface in addition to a nanodroplet size of less than 30 nm are advantageous to facilitate their permeation through the intestinal mucus gel layer and likely also across the absorption membrane [33,34]. The composition of NCs could additionally contribute to an enhanced intestinal uptake of exenatide. The mixture between Capmul<sup>®</sup>MCM, a

medium-chain mono-diglyceride, and Captex® 300, a medium-chain triglyceride, could enhance permeation via the paracellular pathway by opening the tight junctions while keeping the cytotoxicity at its minimum [35,36]. Besides, in addition to its stabilizing effect as a surfactant, Kolliphor® RH40 is an intestinal permeation enhancer known to increase the membrane permeability [37], and it was reported that it may also act as P-glycoprotein (P-gp) inhibitor [38].

Since exenatide has six anionic substructures while only four cationic ones, the lipophilicity of HIPs with the cationic counter ion THA was assumed to be higher compared to those formed with the anionic surfactant DOC. This assumption could be confirmed by the higher solubility of exenatide-THA than exenatide-DOC complexes in the lipophilic phase. Furthermore, the higher potential of exenatide-THA NCs in their membrane permeation behaviour ( $p < 0.01$ ) is in agreement with the higher lipophilic character of this complex. The positive zeta potential of exenatide-THA NCs in comparison to the negatively charged exenatide-DOC NCs might also contribute to their higher membrane permeating properties.

Recently, an enhanced oral bioavailability of exenatide up to 14.0% versus s.c. was achieved with nanoparticles composed of chitosan and poly ( $\gamma$ -glutamic acid) [30]. The results of another research group reported that oral administration of the exenatide-loaded microspheres cross-linked with alginate and hyaluronate had the potential to improve the oral bioavailability of exenatide to 10.15% versus s.c. [6]. The relative oral bioavailability elicited by oral administration of transferrin-exenatide-Zn<sup>2+</sup> nanoparticles was 6.45% which was regarded as a preliminary potential investigation but still needs to be further developed [39]. A recent study by our research group where exenatide was incorporated in self-emulsifying drug delivery system after ion pairing with DOC, showed an oral bioavailability of 14.6% [23] was obtained after oral administration. Exenatide-THA NCs, however, showed an even higher potential reaching a BA<sub>R</sub> of  $27.96 \pm 5.24\%$  (Table 2). These findings also show the great impact of the type of counter ions used for HIP formation on the oral peptide bioavailability. They are in accordance with a previous study demonstrating that the oral bioavailability of octreotide strongly depends on the type of counter ion used for HIP formation. In fact, NCs containing octreotide-deoxycholate led to a 17.9-fold higher oral bioavailability in pigs than octreotide-docusate HIPs [12]. Our study also revealed the potential of cationic surfactants in increasing the lipophilicity of exenatide before being embedded into NCs, which had a great impact on drug release characteristics and intestinal permeability. The developed exenatide-THA NCs holds high promise for oral delivery exceeding the results elicited from preceding reported studies [6,23,30,39–43].

## 6. Conclusion

Within this study, the effectiveness of hydrophobic ion pairing (HIP) of exenatide with a cationic surfactant (THA) in comparison to an anionic surfactant (DOC) was investigated. Optimized HIPs were incorporated into NCs designed for oral delivery. Exenatide-THA NCs demonstrated a 10-fold and 3.3-fold enhancement in intestinal apparent permeability compared to free exenatide and exenatide-DOC NCs, respectively. Following the *ex vivo* findings, the *in vivo* study in rats proved the superiority of the cationic surfactant as the relative oral bioavailability reached  $27.96 \pm 5.24\%$  and was 1.7-fold higher than that obtained with exenatide-DOC. Overall, this study provides substantial new insights for oral delivery of the GLP-1 analogue exenatide.

## Acknowledgment

This work was supported by Technology Grants South East Asia financed by the Austrian Federal Ministry for Science and Research and administered/executed by the OeAD (Austrian Agency for International Cooperation in Education and Research, OeAD-GmbH) and the Austrian Science Fund (FWF): project number ZFP 308390, in addition to the

support of ministry of Human capacities, Hungary (grant 20391-3/2018/FEKUSTRAT), University of Innsbruck, Vice Rectorate for Research and the EU-funded Hungarian grant EFOP-3.6.1-16-2016-00008.

## References

- [1] Y. Shi, et al., Fc-modified exenatide-loaded nanoparticles for oral delivery to improve hypoglycemic effects in mice, *Sci. Rep.* 8 (2018).
- [2] L. Soudry-Kochavi et al., "Pharmacodynamical effects of orally administered exenatide nanoparticles embedded in gastro-resistant microparticles," *Eur. J. Pharm. Biopharm.*, pp. 214-223, 2018.
- [3] R. Ismail, I. Csóka, Novel strategies in the oral delivery of antidiabetic peptide drugs- insulin, GLP 1 and its analogs, *Eur. J. Pharm. Biopharm.* 115 (2017) 257–267.
- [4] Y. Lin, K. Krogh-Andersen, J. Pelletier, H. Marcotte, C. G. Östenson, and L. Hammarström, "Oral delivery of pentameric glucagon-like peptide-1 by recombinant lactobacillus in diabetic rats," *PLoS One*, vol. 11, no. 9, 2016.
- [5] R. Ismail, et al., Synthesis and Statistical Optimization of Poly (Lactic-Co-Glycolic Acid) Nanoparticles Encapsulating GLP1 Analog Designed for Oral Delivery, *Pharm. Res.* 36 (2019) 2620–2629.
- [6] B. Zhang, D. He, Y. Fan, N. Liu, and Y. Chen, "Oral delivery of exenatide via microspheres prepared by cross-linking of alginate and hyaluronate," *PLoS One*, vol. 9, e. 86064, 2014.
- [7] G. Leonaviciute, A. Bernkop-Schnürch, Self-emulsifying drug delivery systems in oral (poly)peptide drug delivery, *Expert Opin. Drug Deliv.* 12 (2015) 1703–1716.
- [8] [https://www.accessdata.fda.gov/drugsatfda\\_docs/label/2019/213051s000lbl.pdf](https://www.accessdata.fda.gov/drugsatfda_docs/label/2019/213051s000lbl.pdf).
- [9] T.A.S. Aguirre, D. Teijeiro-Osorio, M. Rosa, I.S. Coulter, M.J. Alonso, D.J. Brayden, Current status of selected oral peptide technologies in advanced preclinical development and in clinical trials, *Adv. Drug Deliv. Rev.* 106 (2016) 223–241.
- [10] R. Ismail, A. Bocsik, G. Katona, I. Gróf, M.A. Deli, I. Csóka, Encapsulation in polymeric nanoparticles enhances the enzymatic stability and the permeability of the glp-1 analog, liraglutide, across a culture model of intestinal permeability, *Pharmaceutics* 11 (2019) E599.
- [11] J. Griesser, G. Hetényi, M. Moser, F. Demarne, V. Jannin, A. Bernkop-Schnürch, Hydrophobic ion pairing: Key to highly payloaded self-emulsifying peptide drug delivery systems, *Int. J. Pharm.* 520 (2017) 267–274.
- [12] S. Bonengel, et al., Impact of different hydrophobic ion pairs of octreotide on its oral bioavailability in pigs, *J. Control. Release* 273 (2018) 21–29.
- [13] S. Venkata Ramana Rao, J. Shao, Self-nanoemulsifying drug delivery systems (SNEDDS) for oral delivery of protein drugs. I. Formulation development, *Int. J. Pharm.* 362 (2008) 2–9.
- [14] T.N.Q. Phan, I. Shahzadi, A. Bernkop-Schnürch, Hydrophobic ion-pairs and lipid-based nanocarrier systems: The perfect match for delivery of BCS class 3 drugs, *J. Control. Release*. 304 (2019) 146–155.
- [15] T.N.Q. Phan, B. Le-Vinh, N.A. Efiána, A. Bernkop-Schnürch, Oral self-emulsifying delivery systems for systemic administration of therapeutic proteins: science fiction? *J. Drug Target.* 27 (2019) 1017–1024.
- [16] G. Hetényi, J. Griesser, M. Moser, F. Demarne, V. Jannin, A. Bernkop-Schnürch, Comparison of the protective effect of self-emulsifying peptide drug delivery systems towards intestinal proteases and glutathione, *Int. J. Pharm.* 523 (2017) 357–365.
- [17] O. Zupančič, J. Rohrer, H. Thanh Lam, J.A. Grieflinger, A. Bernkop-Schnürch, "Development and *in vitro* characterization of self-emulsifying drug delivery system (SEDDS) for oral opioid peptide delivery", *Drug Dev. Ind. Pharm.* 43 (2017) 1694–1702.
- [18] R. Mahjub, F.A. Dorkoosh, M. Rafiee-Tehrani, A. Bernkop Schnürch, Oral self-nanoemulsifying peptide drug delivery systems: Impact of lipase on drug release, *J. Microencapsul.* 32 (2015) 401–407.
- [19] M.J. Ansari, et al., Enhanced oral bioavailability of insulin-loaded solid lipid nanoparticles: pharmacokinetic bioavailability of insulin-loaded solid lipid nanoparticles in diabetic rats, *Drug Deliv.* 23 (2016) 1927–1929.
- [20] G. Leonaviciute, O. Zupančič, F. Prüfert, J. Rohrer, A. Bernkop-Schnürch, Impact of lipases on the protective effect of SEDDS for incorporated peptide drugs towards intestinal peptidases, *Int. J. Pharm.* 508 (2016) 21–29.
- [21] A. Mahmood, A. Bernkop-Schnürch, SEDDS: A game changing approach for the oral administration of hydrophilic macromolecular drugs, *Adv. Drug Deliv. Rev.* 142 (2018) 91–101.
- [22] J. Griesser, G. Hetényi, H. Kadas, F. Demarne, V. Jannin, A. Bernkop-Schnürch, Self-emulsifying peptide drug delivery systems: How to make them highly mucus permeating, *Int. J. Pharm.* 538 (2018) 159–166.
- [23] C. Menzel, et al., *In vivo* evaluation of an oral self-emulsifying drug delivery system (SEDDS) for exenatide, *J. Control. Release* 277 (2018) 165–172.
- [24] H. Zhou, et al., Microparticle-based lung delivery of INH decreases INH metabolism and targets alveolar macrophages, *J. Control. Release* 107 (2005) 288–299.
- [25] I. Shahzadi, A. Dizdarević, N.A. Efiána, B. Matuszczak, A. Bernkop-Schnürch, Trypsin decorated self-emulsifying drug delivery systems (SEDDS): Key to enhanced mucus permeation, *J. Colloid Interface Sci.* 531 (2018) 253–260.
- [26] A. Bernkop-Schnürch, A. Jalil, Do drug release studies from SEDDS make any sense? *J. Control. Release* 271 (2018) 55–59.
- [27] H.T. Lam, B. Le-Vinh, T.N.Q. Phan, A. Bernkop-Schnürch, Self-emulsifying drug delivery systems and cationic surfactants: do they potentiate each other in cytotoxicity? *J. Pharm. Pharmacol.* 71 (2019) 156–166.
- [28] W.-G. Dai, L.C. Dong, Characterization of physicochemical and biological properties

- of an insulin/lauryl sulfate complex formed by hydrophobic ion pairing, *Int. J. Pharm.* 336 (2007) 58–66.
- [29] A. Rooiantan, J. Farzanfar, S. Mohammadi-Samani, A. Behzad-Behbahani, F. Farjadian, Smart pH responsive drug delivery system based on poly(HEMA-co-DMAEMA) nanohydrogel, *Int. J. Pharm.* 552 (2018) 301–311.
- [30] H.N. Nguyen, et al., The glucose-lowering potential of exendin-4 orally delivered via a pH-sensitive nanoparticle vehicle and effects on subsequent insulin secretion in vivo, *Biomaterials* 32 (2011) 2673–2728.
- [31] S. Hauptstein, F. Prüfert, A. Bernkop-Schnürch, Self-nanoemulsifying drug delivery systems as novel approach for pDNA drug delivery, *Int. J. Pharm.* 487 (2015) 25–31.
- [32] F. Tong, Preparation of exenatide-loaded linear poly(ethylene glycol)-brush poly(L-lysine) block copolymer: potential implications on diabetic nephropathy, *Int. J. Nanomedicine* 12 (2017) 4663–4678.
- [33] O. Zupancic, J. Rohrer, H. Thanh Lam, J.A. Griessinger, A. Bernkop-Schnürch, “Development and in vitro characterization of self-emulsifying drug delivery system (SEDDS) for oral opioid peptide delivery.”, *Drug Dev. Ind. Pharm.* 43 (2017) 1694–1702.
- [34] I. Nardin, S. Köllner, Successful development of oral SEDDS: screening of excipients from the industrial point of view, *Adv. Drug Deliv. Rev.* 487 (2018) 128–140.
- [35] E. H. Holmes, H. Devalapally, L. Li, M. L. Perdue, and G. K. Ostrander, “Permeability Enhancers Dramatically Increase Zanamivir Absolute Bioavailability in Rats: Implications for an Orally Bioavailable Influenza Treatment,” *PLoS One*, vol. 8, e. 61853, 2013.
- [36] J. Keemink, C.A.S. Bergström, Caco-2 Cell Conditions Enabling Studies of Drug Absorption from Digestible Lipid-Based Formulations, *Pharm. Res.* 35 (2018).
- [37] T. Tran, T. Rades, and A. Müllertz, “Formulation of self-nanoemulsifying drug delivery systems containing monoacyl phosphatidylcholine and Kolliphor® RH40 using experimental design,” *Asian J. Pharm. Sci.*, vol.13pp.536-545,2018.
- [38] A. Al-Mohizea, F. Zawaneh, M.A. Alam, F.I. Al-Jenoobi, G.M. El-Maghraby, Effect of pharmaceutical excipients on the permeability of P-glycoprotein substrate, *J. Drug Deliv. Sci. Technol.* 24 (2014) 491–495.
- [39] L. Zhang, et al., Tf ligand-receptor-mediated exenatide-Zn<sup>2+</sup> complex oral-delivery system for penetration enhancement of exenatide, *J. Drug Target.* 26 (2018) 931–940.
- [40] L. Zhang, et al., The use of low molecular weight protamine to enhance oral absorption of exenatide, *Int. J. Pharm.* 547 (2018) 265–273.
- [41] Y. Song, et al., Synthesis of CSK-DEX-PLGA Nanoparticles for the Oral Delivery of Exenatide to Improve Its Mucus Penetration and Intestinal Absorption, *Mol. Pharm.* 16 (2019) 518–532.
- [42] X. Li, et al., The glucose-lowering potential of exenatide delivered orally via goblet cell-targeting nanoparticles, *Pharm. Res.* 32 (2015) 1017–1027.
- [43] C.H. Jin, et al., A new orally available glucagon-like peptide-1 receptor agonist, biotinylated exendin-4, displays improved hypoglycemic effects in db/db mice, *J. Control. Release.* 133 (2009) 172–177.